AGU PUBLICATIONS

JGR

Journal of Geophysical Research: Biogeosciences

RESEARCH ARTICLE
10.1002/2016JG003437

**Key Points:**
- Respiration decreased along with GPP when temperatures exceeded 32°C, and soil moisture was below 0.14 $m^3 m^{-3}$
- The subtropical forest ecosystem turned to a net source of carbon after 2 months of consecutively dry days
- The model captured the water vapor flux variability quite well but overestimated net carbon fluxes during the summer drought

**Supporting Information:**
- Supporting Information S1
- Data Set S1
- Data Set S2

**Correspondence to:**
Z. Xie,
zxie@lasg.iap.ac.cn

**Citation:**
Xie, Z., L. Wang, B. Jia, and X. Yuan (2016), Measuring and modeling the impact of a severe drought on terrestrial ecosystem $CO_2$ and water fluxes in a subtropical forest, *J. Geophys. Res. Biogeosci.*, *121*, 2576–2587, doi:10.1002/2016JG003437.

Received 31 MAR 2016
Accepted 18 SEP 2016
Accepted article online 21 SEP 2016
Published online 11 OCT 2016



# Measuring and modeling the impact of a severe drought on terrestrial ecosystem $CO_2$ and water fluxes in a subtropical forest

**Zhenghui Xie[1], Linying Wang[1,2], Binghao Jia[1], and Xing Yuan[3]**

[1]State Key Laboratory of Numerical Modeling for Atmospheric Sciences and Geophysical Fluid Dynamics, Institute of Atmospheric Physics, Chinese Academy of Sciences, Beijing, China, [2]College of Earth Science, University of Chinese Academy of Sciences, Beijing, China, [3]RCE-TEA, Institute of Atmospheric Physics, Chinese Academy of Sciences, Beijing, China

**Abstract** A severe drought occurred in central and southern China in the summer of 2013. The precipitation dropped to less than 25% of the long-term average, and temperatures were abnormally high for more than 2 months with return periods of 125 years and 301 years, respectively, which induced significant changes in the terrestrial ecohydrological cycle. In this study, the impact of the severe drought on a subtropical forest ecosystem was investigated using measurements from a newly established flux tower and simulations performed by the Community Land Model version 4.5 (CLM4.5). Based on in situ observations, we found that both gross primary production (GPP) and evapotranspiration experienced strong reductions of 76% and 40%, respectively, during the prolonged dry and hot spell. There was an exponential relationship between ecosystem respiration ($R_{eco}$) and temperatures when soil moisture was not too dry, but $R_{eco}$ decreased along with GPP when the temperature exceeded 32°C and soil moisture was below 0.14 $m^3 m^{-3}$. The ecosystem even switched to a net source of carbon in late August. The model captured the variations in water vapor fluxes well, with correlation coefficients $r > 0.88$, but overestimated net ecosystem $CO_2$ exchange because it did not adequately represent carbon fluxes responses to water stress and failed to capture the nonlinear relationship between GPP and $R_{eco}$ during the drought period. The long-term simulation suggested that water availability severely limited carbon sequestration, and both the underlying water use efficiency and inherent water use efficiency reached their maximum values.

## 1. Introduction

Terrestrial ecosystems are a major sink in the global carbon cycle. They sequester carbon during photosynthesis and slow the $CO_2$ increase in the atmosphere [*Le Quéré et al.*, 2013]. Forest ecosystems make a considerable contribution to the net uptake of carbon into the terrestrial biosphere [*Beer et al.*, 2010; *Bonan*, 2008; *Cox et al.*, 2013; *Pan et al.*, 2011]. However, severe regional extreme events, such as droughts and heat waves, have become more frequent under a changing climate and their trend is expected to continue for the foreseeable future [*Dai*, 2013; *Wang et al.*, 2014]. Their occurrence may partially offset carbon sinks or even cause net losses in carbon stocks, thereby releasing $CO_2$ to the atmosphere [*Zeng et al.*, 2005]. Therefore, it is essential to study the impact of droughts on the terrestrial carbon cycle, which can improve our understanding of carbon-climate interactions [*Reichstein et al.*, 2013].

The impact of droughts on ecosystem water and carbon balances has been extensively investigated using in situ observations. It has been found that both gross primary production (GPP) and ecosystem respiration ($R_{eco}$) declined considerably when soil moisture dropped below a critical threshold during the 2003 European drought [*Granier et al.*, 2007]. Similar findings were also reported in a temperate broad-leaved forest in 1995 [*Baldocchi*, 1997] and in a New Zealand tussock grassland from 1998 to 1999 [*Hunt et al.*, 2002]. However, the ecosystem response to droughts in humid climate zones is less well documented because predicting drought in terms of time, duration, and intensity is more difficult [*Baldocchi*, 2008]. Droughts may have dramatic effects on the carbon exchange in these regions. For example, moderate droughts may result in additional carbon uptake through increased photosynthesis and reduced respiration in tropical and humid temperate forests because there is less rainfall associated with fewer clouds and more available light [*Saleska et al.*, 2003]. However, severe droughts lead to large reductions in carbon uptake because photosynthesis is restricted in a subtropical evergreen forest ecosystem [*Wen et al.*, 2010].

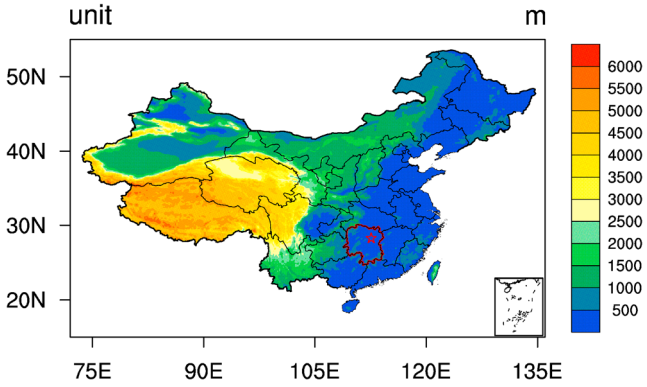


**Figure 1.** The location of the study site and topography. The area outlined in red is Hunan Province, and the red star represents Ningxiang experimental station.

In addition to in situ measurements, ecosystem modeling has also been used to understand the responses of the carbon and water cycles to droughts [*Keenan et al*., 2009; *Krinner et al*., 2005; *Reichstein et al*., 2007]. Coupled biogeochemical cycle (BGC)-general circulation models are some of the most important approaches and tools for studying biosphere-atmosphere interactions. They can be used to predict global and regional alterations in terrestrial ecosystems and identify potential positive feedback loops [*Sakaguchi et al*., 2011]. However, there is limited confidence in simulating the biosphere's response to climate extremes due to large uncertainties in the dynamics and physical parameterizations associated with climate extremes [*Loreto and Centritto*, 2008].

During the summer of 2013, a subtropical forest located in southern China experienced an extreme drought [*LeComte*, 2014] when the July–August temperature was up to 2°C warmer than normal, and the total precipitation was 236 mm below normal for the 2 months, which was only 13% of the average [*Jia et al*., 2015]. It was a "flash drought" event due to its rapid development, unusual intensity, and devastating impacts [*Yuan et al*., 2015]. Summer is the major growing season in this area, and the vegetation productivity, especially for the forest, is susceptible to drought [*Van der Molen et al*., 2011]. However, the drought-responsive mechanisms in subtropical forest ecosystems are still not clear.

In this study, we used both the observations from a newly established flux tower, and a process-based land surface model to investigate the influence of the 2013 summer drought on ecosystem $CO_2$ and water fluxes in a subtropical forest in southern China. We focused on the changes in terrestrial carbon and water cycles under drought conditions, and the model performance in drought extremes in subtropical forest. Furthermore, this study demonstrated how strong the link was between carbon and water cycles when they responded to drought.

## 2. Methods

### 2.1. Study Site

Ningxiang field experimental observatory (NX, 112°34′E, 28°20′N, 110 m above sea level) was established over a hilly region in Hunan Province of Southern China in August 2012 (Figure 1 [*Liu et al*., 2013; *Jia et al*., 2015]). The climate in this area is subtropical, with an annual mean rainfall of 1420 mm and a mean temperature of 17°C. A 20 m flux tower was set up after considering the homogeneity of the terrain and land cover. The local terrain is relatively flat, and the experimental site is mainly surrounded by evergreen broadleaf trees (about 1 $km^2$). The trees are over 40 years old, the dominant species include *Cinnamomum camphora* and *Pinus massoniana*, and the average canopy height is about 7 m.

### 2.2. $CO_2$ and $H_2O$ Fluxes, and Meteorological Data

The $CO_2$ and $H_2O$ fluxes were measured continuously from 1 January to 31 December 2013 using the eddy covariance (EC) method, by instruments (EC150, Campbell Scientific, Logan, UT, USA) installed 17.5 m above the ground. Solar radiation components were measured at the same height. These fluxes were recorded by a CR3000 data logger (Campbell Scientific) with a 10 Hz sampling frequency. They were averaged every 30 min. Synchronous meteorological observation data included precipitation, air temperature, relative humidity, soil temperature, and soil water content, which were collected by a CR1000 data logger (Campbell Scientific) and recorded every 10 min. Further details about the instruments can be obtained from *Liu et al*. [2013].

The raw fluxes for $CO_2$, water, and heat were calculated and converted every 30 min using algorithms for three-dimension coordinate rotation [*Liu et al*., 2006; *Wilczak et al*., 2001], density fluctuations correction

[*Webb et al*., 1980], and the average value test method [*Zhu et al*., 2006]. After these corrections, only 61% of net ecosystem $CO_2$ exchange (NEE) data were available compared to the raw data. Therefore, a gap-filling procedure, following the marginal distribution sampling method [*Reichstein et al*., 2005], was adopted in this study.

The method outlined by *Reichstein et al*. [2005] was used to partition NEE into $R_{eco}$ and GPP. An exponential regression model with a reference temperature ($T_{ref}$) of 10°C and a regression parameter ($T_0$) of –46.02°C from *Lloyd and Taylor* [1994] was used to estimate $R_{eco}$ according to equation (1):

$$R_{eco}(t) = R_{ref}(t)e^{E_0(1/(T_{ref}-T_0)-(1/(T(t)-T_0))} \quad (1)$$

where $R_{ref}$, the base respiration at $T_{ref}$, is a temperature independent parameter that varies temporally and $E_0$ is the short-term temperature sensitivity of $R_{eco}$, which was introduced to avoid the bias introduced by confounding factors [*Reichstein et al*., 2005]. GPP is the difference between NEE and $R_{eco}$. More detailed information about the quality-control, gap-filling and flux-partitioning processes can be found in *Jia et al*. [2015].

### 2.3. Modeling Approach

The process-based land surface model CLM4.5 [*Oleson et al*., 2013] is the terrestrial component of the Community Earth System Model version 1.2. It includes biogeophysical, hydrological cycle, and biogeochemical components and can estimate soil-plant-atmosphere carbon, water, and energy fluxes. The land surface is represented as nested subgrid land cover types consisting of glacier, lake, wetland, urban, and vegetation land. The vegetation land unit is further divided into bare ground (i.e., Bare) and 15 plant function types (PFTs). Each PFT has its own leaf and stem parameters, root distribution, and canopy height. The terrestrial carbon cycle in CLM4.5 can be described as follows: the uptake of carbon from the atmosphere via photosynthesis (i.e., GPP), the storage of carbon in biomass and soils, and the release of carbon back to the atmosphere through plant (autotrophic) and microbial (heterotrophic) respiration [*Hudiburg et al*., 2013]. Net ecosystem productivity is the difference between GPP and ecosystem respiration (i.e., the sum of autotrophic respiration and heterotrophic respiration). The plant physiological response to drought stress was modeled in two ways [*Keenan et al*., 2010; *Oleson et al*., 2013]. The first method is to constrain the stomatal conductance directly by reducing the minimum conductance with the soil water stress factor $\beta_t$ (which ranged from 0 to 1):

$$g_s = m\frac{A_n}{c_s/P_{atm}}h_s + b\beta_t \quad (2)$$

where $g_s$ is the stomatal conductance, $m$ is a plant functional-type dependent parameter, $A_n$ is the leaf net photosynthesis, $c_s$ is the $CO_2$ partial pressure at the leaf surface, $P_{atm}$ is the atmospheric pressure, $h_s$ is the leaf surface humidity, and $b$ is the minimum stomatal conductance. The limitation in stomatal conductance can further affect the available $CO_2$ for photosynthesis.

The second method is to impose stress on photosynthesis by reducing $V_{cmax}$ with $\beta_t$:

$$V_{cmax} = V_{cmax} \times \beta_t \quad (3)$$

where $V_{cmax}$ is the maximum rate of carboxylation. Reduction in photosynthesis can also limit the demand for $CO_2$ and indirectly influence the conductance process.

All simulations in this study were performed using CLM4.5 with the prognostic carbon and nitrogen dynamics taken from the terrestrial biogeochemical model (Biome-BGC4.1.2 [*Thornton and Rosenbloom*, 2005]), hereafter referred to as CLM4.5-CN. The default meteorological forcing data were from the China Meteorological Administration (CMA) National Meteorological Information Center (hereafter referred to as CMA; http://data.cma.cn [*Jia et al*., 2013; *Shi et al*., 2011]). They include precipitation, temperature, wind, humidity, pressure, and downward shortwave radiation data. The CMA forcing data have a high spatial resolution of 0.0625° and an hourly interval. In the CLM4.5 model, the maximum porosity was reduced from 0.489 to 0.289 to avoid a systematic wet bias for the soil moisture, and the land cover was specified as broadleaf evergreen tree-temperate cover (i.e., BEM Tr) with default PFT parameters.

We ran CLM4.5-CN offline (i.e., not coupled to an active atmospheric model) with the prescribed vegetation cover and conducted two sets of simulations. These involved changing the forcing data due to its important effects on the performance of the ecohydrology simulation. In the first simulation, the 4 year (2009–2012) CMA

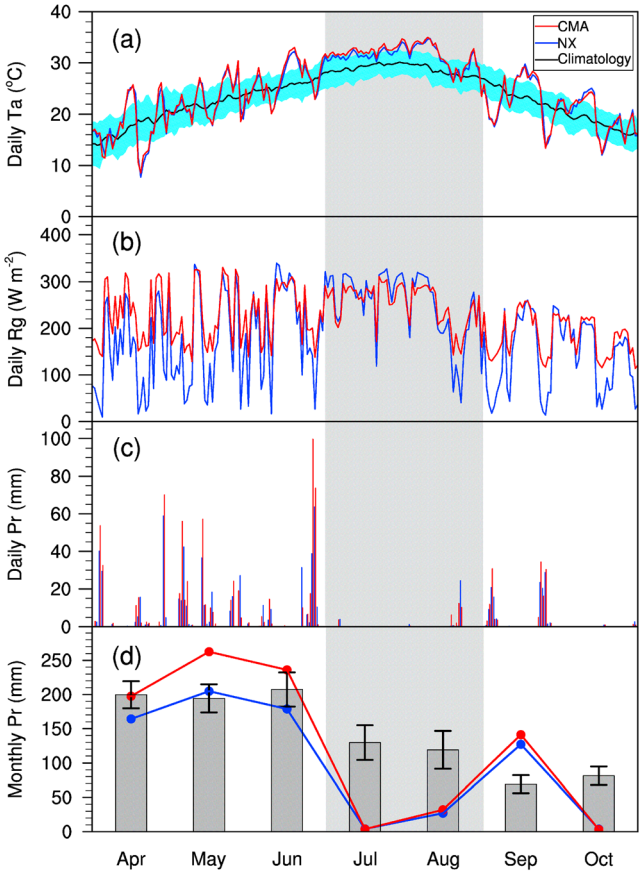


**Figure 2.** Time series of daily mean (a) air temperature ($T_a$, blue and red lines are for in situ (NX) and CMA forcing (CMA) data, respectively; black line represents the climatology data, and the blue band indicates one standard deviation from the historical data); (b) solar radiation ($R_g$); (c) precipitation ($P_r$); and (d) monthly mean $P_r$ and climatology (grey bar with 95% confidence interval, which is calculated by $p = 0.975$ for two-tailed test).

meteorological forcing data were repeatedly used to drive the spin-up simulation for 1200 years to establish equilibrium states for the carbon and nitrogen pools and fluxes. Based on the initial states from the spin-up simulation, the simulation named "CLM-CMA" was run using the CMA forcing data from 2009 to 2013. In the second simulation, hereafter referred to as "CLM-NX," all conditions were identical to CLM-CMA, with the exception that the meteorological data for 2013 were based on the local eddy covariance tower measurements. We also conducted a climatological simulation to reproduce the climatology of the ecosystem response. As the CMA forcing data only covered 5 years, we merged observations from the local meteorological station with data from multiple satellites and reanalysis data to create a new meteorological forcing data set. This was then used to run the model during the period of 1979–2012.

## 3. Results

### 3.1. Characteristics of the 2013 Summer Drought

Figure 2 shows the major meteorological conditions at the NX site during the 2013 growing season (April–October). The results showed that the daily mean in situ air temperature ($T_a$, Figure 2a) ranged from 7.7°C to 34.7°C, and mean $T_a$ for July–August (31.2°C) was 2.4°C higher than normal (28.8°C) and was the most severe heat wave in recorded history (1979–2013, Figure 3b). There were 67 consecutive days (28 June to 2 September) during which the daily maximum temperature exceeded the average temperature by 5°C. Estimated by the generalized extreme value method [*Kotz and Nadarajah*, 2000], the 2013 heat wave appeared to be a 301 year extreme event. The CMA temperature data agreed with the in situ air temperature quite well, with a correlation coefficient ($r$) of 0.99 and a root-mean-square error (RMSE) of 0.8°C. In contrast, the difference in downward shortwave radiation ($R_g$) between the in situ measurements and the CMA forcing data was larger, with a correlation of 0.94 and a RMSE of 54.1 W m$^{-2}$. The CMA $R_g$ data had smaller variabilities and overestimated low values compared to the in situ measurements. A large bias in $R_g$ affected the plant growth simulation.

The cumulative in situ precipitation for the growing season in 2013 was 710 mm, which was significantly lower than the climatology (1001 mm). In addition, there were only 4.1 mm and 27.0 mm of rainfall in July and August, respectively, which were only about 3.1% and 22.7% of their expected climatological values (129.7 mm and 119.2 mm, respectively) (Figure 2c). The 2013 summer drought was also an extreme event (125 year return period) (Figure 3a). The CMA precipitation data also agreed well with the in situ measurements in terms of temporal variation ($r = 0.83$). The high correlations between in situ measurements and the CMA forcing data indicated the high quality of the two data sets and ensured the accuracy of meteorological forcing for land surface model simulations by CLM4.5.

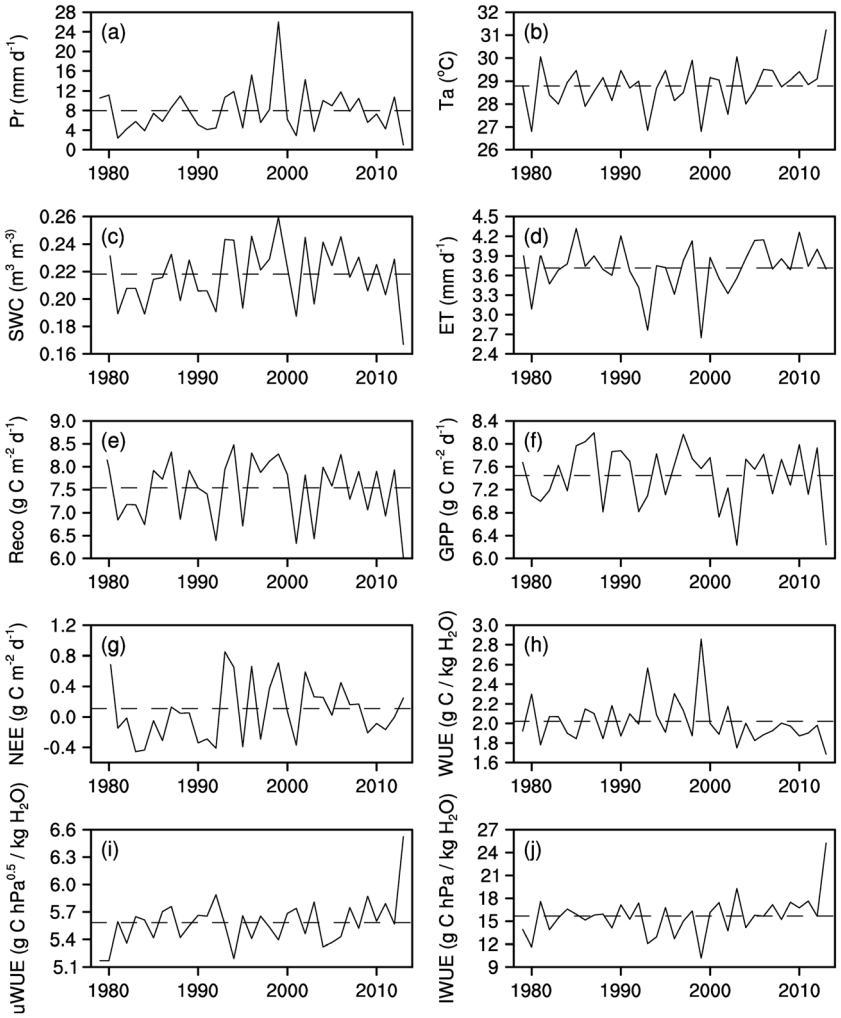


**Figure 3.** Interannual changes of (a) precipitation ($P_r$), (b) air temperature ($T_a$), (c) soil water content (SWC), (d) evapotranspiration (ET), (e) ecosystem respiration ($R_{eco}$), (f) gross primary production (GPP), (g) net ecosystem $CO_2$ exchange (NEE), (h) water use efficiency (WUE), (i) underlying water use efficiency (uWUE), and (j) inherent water use efficiency (IWUE) for July–August from 1979 to 2013 at Ningxiang. Figures 3a and 3b are observed data, and Figures 3c–3j are simulated results.

### 3.2. Effect of Drought on Water Vapor and $CO_2$ Fluxes

The meteorological drought (precipitation deficit) during July–August led to a severe agricultural drought: in situ soil water content (SWC) at 5 cm declined rapidly from 0.35 $m^3\,m^{-3}$ at the end of June to 0.12 $m^3\,m^{-3}$ on 22 August, which was much lower than the expected climatological values (Figure 4a). The simulated SWC captured the temporal variations in the in situ observations quite well with a correlation coefficient of $r = 0.93$ (Table 1). The systematic overestimation (RMSE $> 0.09\,m^3\,m^{-3}$, not shown) was alleviated by the modified soil porosity, which is based on an empirical relationship with soil texture. However, the model did not capture the magnitude of the decline in soil moisture during August. This was mainly associated with very low soil water potential and may have affected the ecosystem physiological response simulation in late August. In the CLM4.5 model, soil moisture affected stomatal conductance directly by a soil water stress function where one represented no water stress and zero represented severe water stress. During the drought period, the water stress factor decreased considerably (Figure 4b), which indicated that the model imposed more stress on plant growth during the simulation. Consequently, the simulated canopy transpiration, which is a significant component of evapotranspiration (ET) in forests [*Reichstein et al.*, 2007; *Schlesinger and Jasechko*, 2014], also decreased significantly due to water stress. It should be noted that the variation in ET during the 2013 summer drought was within one standard deviation of the climatology data, and that the average ET in July–August of 2013 was similar to the long-term average because water deficits reduced

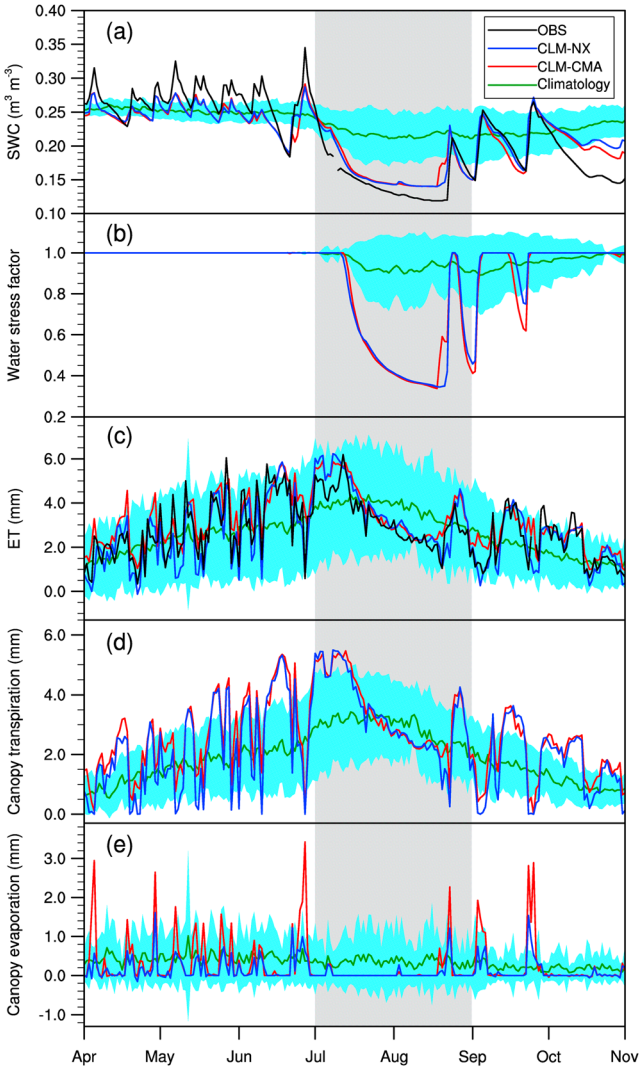


**Figure 4.** Time series of daily mean (a) soil water content (SWC), (b) water stress factor, (c) total evapotranspiration (ET), (d) canopy transpiration, and (e) canopy evaporation during the 2013 growing season for the in situ observations (OBS), the CLM-CMA and CLM-NX simulations, and the climatological simulation (Climatology, the blue band indicates one standard deviation from the historical data).

the ET values, whereas high temperature increased them. Figure 4c shows that in situ ET also decreased from 6.2 mm $d^{-1}$ on 12 July to 1.0 mm $d^{-1}$ on 20 August. The CLM4.5 model reproduced well the ET seasonal cycle with a high $r$ (>0.85) and a low RMSE (<0.8 mm $d^{-1}$). In addition, apparent differences in canopy evaporation from the two simulations can be seen in Figure 4e, and this might be related to the differences in radiation and precipitation (Figures 2b and 2d).

The dynamics of the ecosystem $CO_2$ fluxes are shown in Figure 5. The mean values for NEE, $R_{eco}$, and GPP during the growing season were $-1.6 \pm 2.4$, $6.2 \pm 1.7$, and $7.8 \pm 2.9$ g C $m^{-2}$ $d^{-1}$, respectively. The NEE represents the balance between carbon uptake and release, and maximum carbon uptake occurred on 12 June (–7.4 g C $m^{-2}$ $d^{-1}$). During the summer drought period, carbon uptake decreased as the soil water content fell, and the ecosystem even became a net source of $CO_2$, with a rate of 4.3 g C $m^{-2}$ $d^{-1}$ on 23 August. The NEE magnitude also decreased from 12.2 to 8.0 g C $m^{-2}$ $d^{-1}$. *Lloyd and Taylor* [1994] pointed out that $R_{eco}$ was mainly related to temperature, while the respiration rate at reference conditions should vary seasonally to avoid the bias introduced by confounding factors in seasonal data, such as plant physiological patterns, soil moisture [*Joo et al.*, 2012], decomposition, and/or soil microbial growth dynamics [*Reichstein et al.*, 2005]. The soil water deficit meant that the variation in $R_{eco}$ (Figure 5b) was not consistent with the change in temperature during the drought period (Figure 2a). For example, $R_{eco}$ increased as the temperature warmed during April–June but decreased in July and August. However, there was light rain (about 4 mm) on 7 July, which led to a

**Table 1.** Summary Statistics for the Two Simulations Compared to In Situ Observations During the 2013 Growing Season[a]

| Case | Statistics | SWC | ET | NEE | $R_{eco}$ | GPP |
|---|---|---|---|---|---|---|
| CLM-CMA | $r$ | 0.93 | 0.85 | 0.22 | 0.58 | 0.49 |
| | RMSE | 0.02 | 0.80 | 2.64 | 1.80 | 2.65 |
| CLM-NX | $r$ | 0.93 | 0.89 | 0.76 | 0.64 | 0.86 |
| | RMSE | 0.02 | 0.70 | 2.20 | 1.80 | 1,79 |

[a]The letter $r$ is the correlation coefficient. RMSE is the root-mean-square error, and the units for soil water content (SWC), evapotranspiration (ET), net ecosystem $CO_2$ exchange (NEE), ecosystem respiration ($R_{eco}$), and gross primary production (GPP) are $m^3$ $m^{-3}$, mm $d^{-1}$, g C $m^{-2}$ $d^{-1}$, g C $m^{-2}$ $d^{-1}$, and g C $m^{-2}$ $d^{-1}$, respectively.

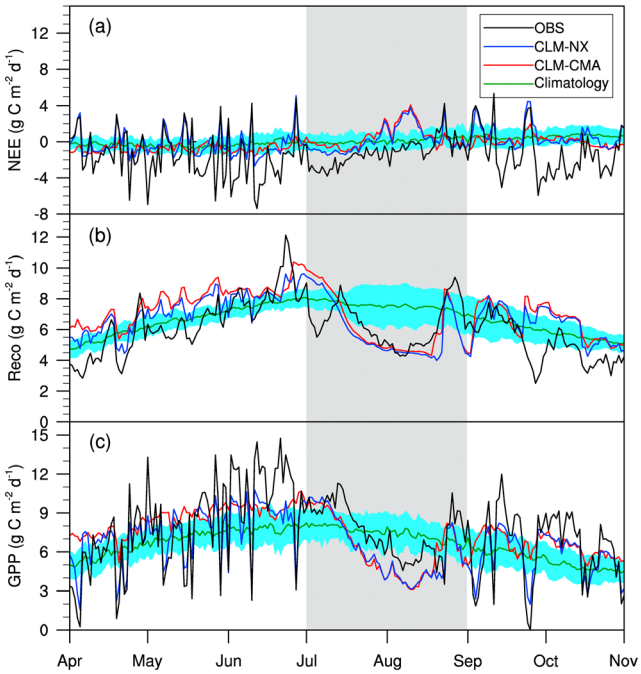


**Figure 5.** Time series of daily mean (a) net ecosystem $CO_2$ exchange (NEE), (b) ecosystem respiration ($R_{eco}$), and (c) gross primary production (GPP) during the 2013 growing season for the in situ observations (OBS), the CLM-CMA and CLM-NX simulations, and the climatological simulation (Climatology, the blue band indicates one standard deviation from the historical data).

conspicuous increase in $R_{eco}$. Before the summer drought period, GPP peaked at 14.7 g C $m^{-2}$ $d^{-1}$ on 21 June, but in August, GPP decreased to 3.5 g C $m^{-2}$ $d^{-1}$ due to the soil water deficit and the increasing vapor pressure deficit (VPD). Both $R_{eco}$ and GPP were far below the expected average values, especially in August. The average $R_{eco}$ and GPP in July–August of 2013 reached the recorded minimums (Figures 3e and 3f) with return periods of 45 years and 41 years, respectively.

Modeled NEE in the CLM-NX simulation had a better agreement with observations compared with CLM-CMA (Figure 5a and Table 1, $r$ increased from 0.22 to 0.76). However, even when forced by in situ observations, the NEE was less well simulated by CLM4.5 during the drought period (Table 2, $r = 0.55$) than in the wet period ($r = 0.83$). CLM-NX also did not capture the temporal variation in $R_{eco}$ well ($r = 0.57$), especially with regards to its response to vapor deficits. In particular, GPP was relatively low (Figure 5c) and both simulations underestimated GPP in August. In the CLM4.5 simulation, $R_{eco}$ included heterotrophic respiration (HR) and autotrophic respiration (AR). HR is the decomposition of litter and soil organic matter, and AR is the sum of maintenance respiration (MR) and growth respiration (GR), where MR supports the metabolic costs of existing live leaves, stems, and roots and GR is the additional carbon cost needed for new plant growth [*Oleson et al.*, 2013]. The time series for these components are shown in Figure 6. Heterotrophic respiration decreased during the drought period but considerably increased after the drought (Figure 6a). In early July, MR kept high values, contributing to high AR, which resulted in an overestimation of $R_{eco}$. In late August, HR had comparable values to AR, and they contributed equally to the low $R_{eco}$ values. The AR simulation with in situ radiation forcings performed better (Figure 6b), which was similar to the improved $R_{eco}$ simulation (Figure 5b), and was mainly due to the better simulation of GR (Figure 6c).

### 3.3. Water Stress Effects on Vegetation Growth

Figure 7 shows the relationship between $R_{eco}$ and air temperature under different soil moisture conditions (SWC $< 0.14$, $0.14 \leq$ SWC $< 0.21$, $0.21 \leq$ SWC $< 0.26$, and SWC $\geq 0.26$, unit in $m^3$ $m^{-3}$). A clear exponential relationship was found when SWC $> 0.14$ $m^3$ $m^{-3}$. $R_{eco}$ was higher in wet soil than in dry soil, especially at high

**Table 2.** Summary Statistics for the CLM-NX Experiment Compared to In Situ Observations During the Wet and Dry (July–August) Periods in the 2013 Growing Season[a]

| Period | Statistics | SWC | ET | NEE | $R_{eco}$ | GPP |
|---|---|---|---|---|---|---|
| Wet | $r$ | 0.90 | 0.88 | 0.83 | 0.80 | 0.91 |
| | RMSE | 0.03 | 0.69 | 2.29 | 1.51 | 1.80 |
| Dry | $r$ | 0.91 | 0.90 | 0.55 | 0.57 | 0.87 |
| | RMSE | 0.02 | 0.72 | 1.97 | 1.53 | 1.75 |

[a]The letter $r$ is the correlation coefficient. RMSE is the root-mean-square error, and the units for soil water content (SWC), evapotranspiration (ET), net ecosystem $CO_2$ exchange (NEE), ecosystem respiration ($R_{eco}$), and gross primary production (GPP) are $m^3$ $m^{-3}$, mm $d^{-1}$, g C $m^{-2}$ $d^{-1}$, g C $m^{-2}$ $d^{-1}$, and g C $m^{-2}$ $d^{-1}$, respectively.

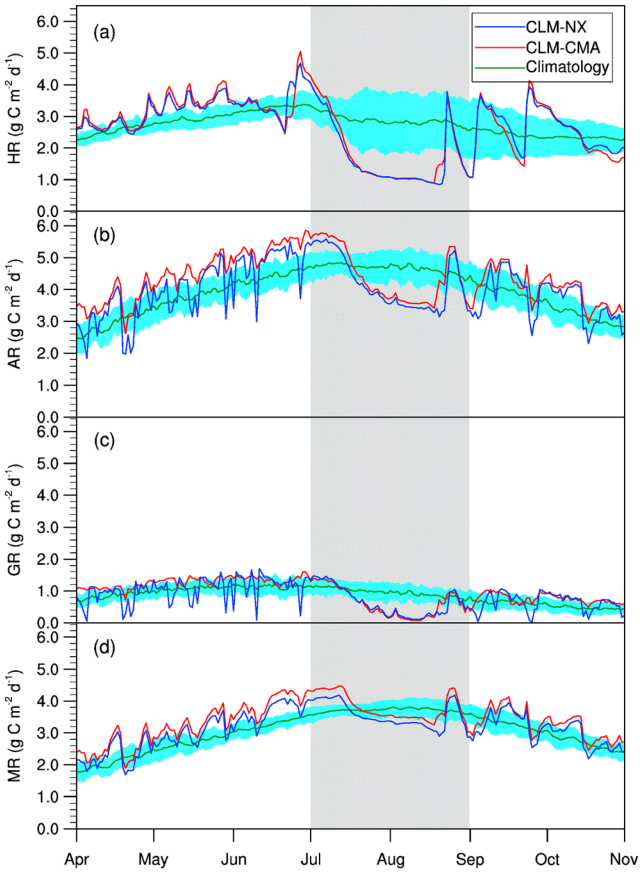


**Figure 6.** Time series of daily mean (a) heterotrophic respiration (HR), (b) autotrophic respiration (AR, i.e., MR + GR), (c) total growth respiration (GR), and (d) maintenance respiration (MR) during the 2013 growing season for the CLM4.5 simulation and the climatological simulation (Climatology, the blue band indicates one standard deviation from the history data).

temperatures. When soil water content was below 0.14 $m^3 m^{-3}$, $R_{eco}$ changed little as the temperature rose. The CLM4.5 captured the exponential relationship between $R_{eco}$ and $T_a$ well under wet soil conditions. Under very dry soil conditions, simulated $R_{eco}$ had low values instead of increasing as the temperature rose.

Before and after the drought period, the actual observations and model simulations showed that there were no clear relationships between $R_{eco}$/GPP and SWC (Figure 8). However, during the summer drought, water availability became the main limiting factor, and both $R_{eco}$ and GPP declined as soil moisture decreased. The decline trend was captured by the model, although the shape was slightly different from the observed data. There was some noise in the observation at the very low end of the soil moisture range where the exponential relationship between carbon fluxes and water stress did not hold.

We also investigated the relationship between $R_{eco}$ and GPP using monthly observed and modeled data. There was a significant linear relationship between $R_{eco}$ and GPP (Figure 9a). However, there were some outliers for August and September (crosses) because of seasonal drought effects. Similar results were found by *Sun et al.* [2006] for a midsubtropical planted forest in southeastern China. In this study, the simulated regression coefficient (excluding August and September) was similar to the in situ observations, but the model failed to reproduce the nonlinear relationship during the drought (Figure 9b).

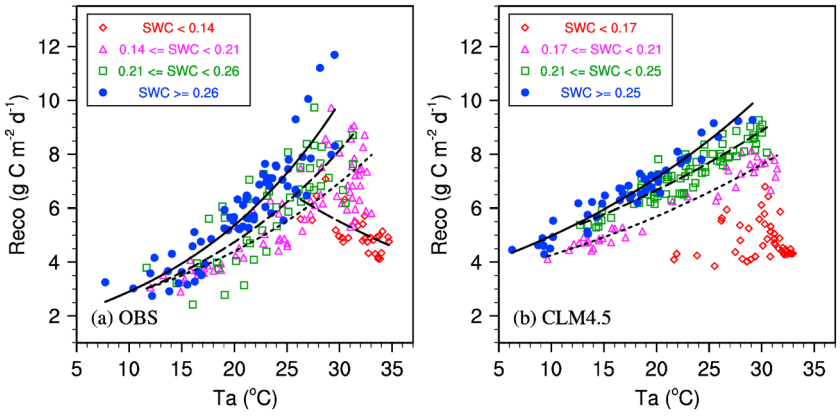


**Figure 7.** The effect of daily air temperature on ecosystem respiration ($R_{eco}$) under different soil moisture conditions from April to October for (a) the in situ observations (OBS) and (b) the CLM-NX simulation (CLM4.5).

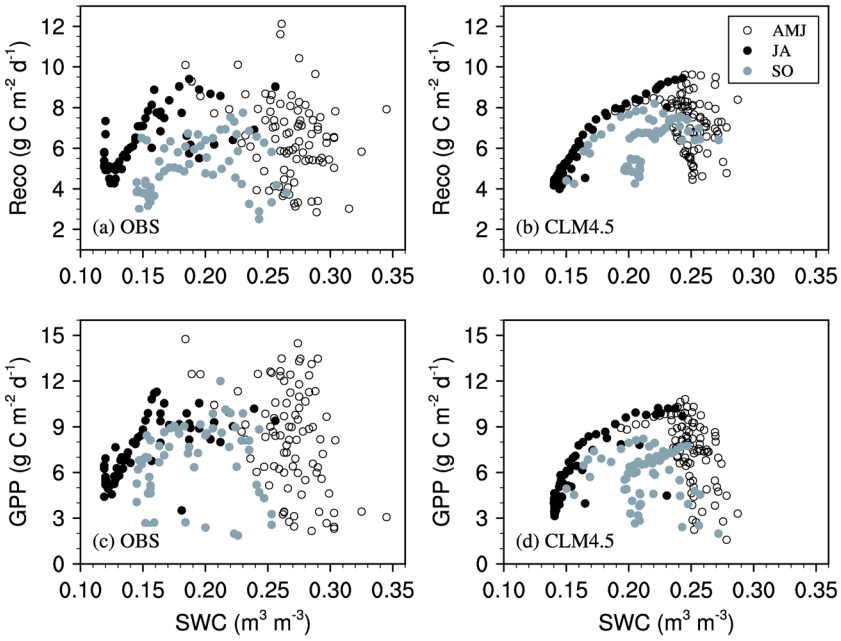


**Figure 8.** The relationship between soil moisture (SWC) versus (a, b) ecosystem respiration ($R_{eco}$) and (c, d) GPP over different periods (April-May-June, AMJ; July–August, JA; and September–October, SO) during the 2013 growing season for (Figures 8a and 8c) the in situ observations (OBS) and (Figures 8b and 8d) the CLM-NX simulation (CLM4.5).

Water is one of the major drivers of the forest ecosystem, and the carbon cycle is closely associated with the water cycle partly via stomatal behavior. At the ecosystem level, water use efficiency has been used to quantify the trade-off between the amount of assimilated carbon and water loss. It therefore reflects the coupled relationship between carbon and water [*Law et al.*, 2002; *Yu et al.*, 2008]. In this study, we assessed three formulations for water use efficiency under different assumptions, i.e., the original water use efficiency (WUE = GPP/ET) [*Cowan and Farquhar*, 1977], the inherent water use efficiency (IWUE = GPP · VPD/ET) [*Beer et al.*, 2009], and the underlying water use efficiency (uWUE = GPP · $VPD^{0.5}$/ET) [*Zhou et al.*, 2015]. WUE is defined as the amount of carbon gained per unit of water loss at the ecosystem level; IWUE is derived by considering the diffusion process for $CO_2$ and water leaving or entering the leaf; and uWUE is based on IWUE and a simple stomatal model. The variation in WUE was quite small during the summer drought, and there was a slight decline compared to the simulated climatology (Figures 10a and 3h). However, both uWUE and IWUE experienced a significant increase and reached their recorded

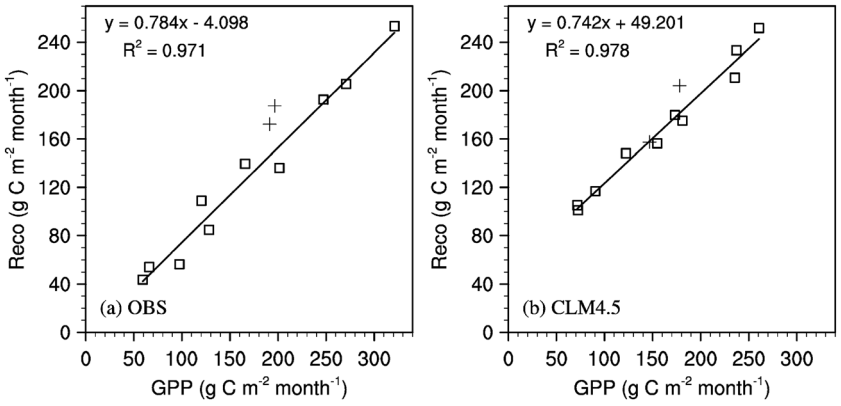


**Figure 9.** The relationship between ecosystem respiration ($R_{eco}$) and gross primary production (GPP) on a monthly scale in 2013 for (a) the in situ observations (OBS) and (b) the CLM-NX simulation (CLM4.5). The crosses represent the values for August and September, and blank squares represent the values for other months. The solid line represents the regression line but does not include the data for August and September.

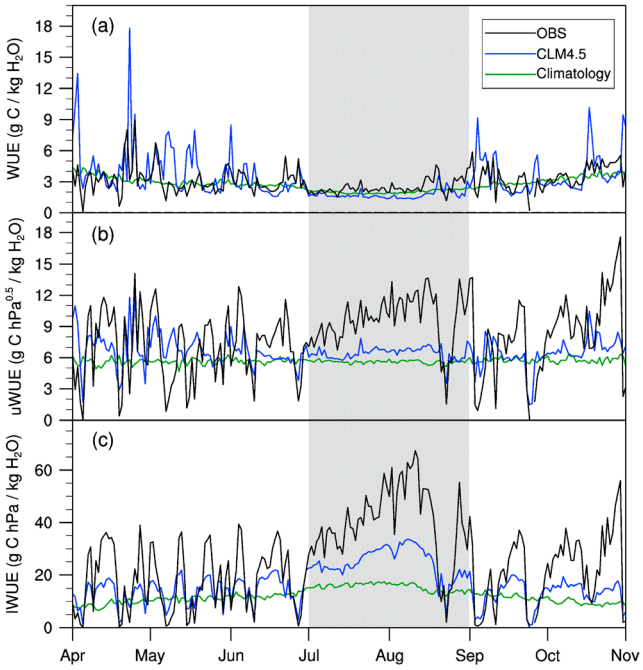


**Figure 10.** Time series for the (a) water use efficiency (WUE), (b) underlying water use efficiency (uWUE), and (c) inherent water use efficiency (IWUE) daily means during the 2013 growing season for the in situ observations (OBS), the CLM-NX simulation (CLM4.5), and the climatological simulation (Climatology, the blue band indicates one standard deviation from the historical data).

maximums (Figures 10b and 10c and 3i and 3j) if the nonlinear effect of VPD was taken into account. The model also reproduced the decrease in WUE and increase in uWUE and IWUE but underestimated all three WUEs during the water stressed period.

## 4. Conclusions and Discussion

In this study, the impact of the 2013 summer heat and drought on a mixed evergreen ecosystem in southern China was investigated using both ground-based observations from a flux tower and simulations by the land surface model CLM4.5 with the prognostic carbon and nitrogen dynamics. Based on the July–August precipitation and air temperature data from 1979 to 2013, the ecosystem experienced its most severe drought and heat wave with return periods of 125 years and 301 years, respectively. The precipitation dropped to 23% of the mean precipitation, and the temperature was abnormally high for 67 days during the summer. This led to the highest recorded reductions in SWC. Due to severe water stress in the soil and atmosphere, plant photosynthesis was clearly restricted in July and August and reached the recorded minimums.

Ecosystem respiration decreased along with GPP instead of accelerating as the temperature rose. $R_{eco}$ increased exponentially with the increase in temperature when soil water content was plentiful but changed little under dry soil conditions ($<0.14\,m^3\,m^{-3}$). As a balance between carbon uptake and release, NEE's magnitude also experienced a large reduction from 12.2 to 8.0 g C $m^{-2}\,d^{-1}$ and the ecosystem even switched to being a net source of carbon with a rate of 4.3 g C $m^{-2}\,d^{-1}$ on 23 August. Moreover, dry soil conditions limited plant water uptake, led to a decrease in stomatal conductance, and altered the coupling between water and carbon fluxes.

The CLM4.5 model produced accurate estimations of SWC ($r = 0.93$) and ET ($r > 0.85$) variability during the growing season, and its ability to reproduce the carbon fluxes improved substantially ($r = 0.76$ for NEE) when the atmospheric forcing data were replaced with in situ observations. However, the GPP simulated by CLM4.5 was smaller than the in situ observed GPP during the drought period, which led to the overestimation of the release of carbon to the atmosphere. The simulated $R_{eco}$ values were also overestimated in early July and did not capture the reduction shown in the observed values. The mismatch between the observed and simulated values was complex as both the in situ data and the models contained some uncertainties. The observed and predicted relationship comparison among GPP, $R_{eco}$ and water stress showed that the model had some difficulties in representing the response of carbon fluxes to water stress and failed to capture the nonlinear relationship between GPP and $R_{eco}$. This suggests insufficient understanding of plant responses to water stress and the necessity of improving the model parameterizations [*Keenan et al.*, 2010]. However, the uncertainty present in the in situ eddy covariance measurements should also be considered. As in situ $R_{eco}$ was difficult to measure directly, we assumed that the nighttime NEE eddy covariance measurements would be equal to $R_{eco}$ at night and compared them to in situ $R_{eco}$ estimates and simulated $R_{eco}$ values to evaluate the plausible uncertainty (Figure 11). We found that the in situ $R_{eco}$, which was estimated from an empirical formula based on the hypothesis that respiration is a nonlinear function of temperature, captured the

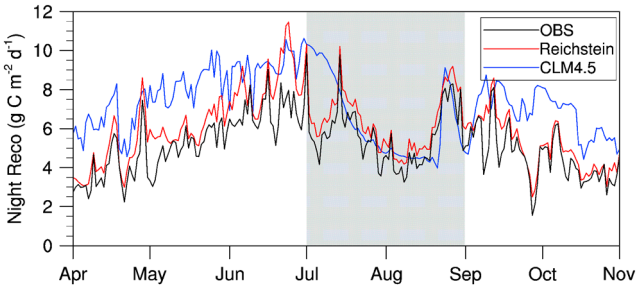


**Figure 11.** Time series for the nighttime respiration ($R_{eco}$) daily mean during the 2013 growing season: (a) NEE eddy covariance measurements, which can be termed as observations (OBS), (b) in situ $R_{eco}$, as estimated by the *Reichstein et al.* [2005] method (Reichstein), and (c) CLM-NX-simulated $R_{eco}$ (CLM4.5). For both the in situ and model nighttime values, the in situ downward shortwave radiation ($R_g$) of less than 0.01 was used as a reference.

nighttime NEE variability quite well ($r = 0.92$). While in CLM4.5, the calculation of $R_{eco}$ was rather complicated as it took various environmental factors and different plant growth processes (e.g., heterotrophic respiration and autotrophic respiration) into account. Therefore, the $R_{eco}$ simulation by CLM-NX was not very accurate ($r = 0.51$), and a large uncertainty in the physical representation of ecological process still existed.

The summer drought played an important role in the target ecosystem's carbon and water cycle, and the reduced carbon fluxes were associated with both the water deficit and high temperature. However, this study only quantified the short-term consequences of summer heat and drought on the terrestrial carbon cycle. The immediate and time-lagged responses (e.g., mortality or fire) need further investigation. Other in situ measurements with longer records are being collected to investigate the drought-carbon coupling more comprehensively. The related ecohydrological parameterizations in land surface models also need to be improved if they are to represent processes across scales.

**Acknowledgments**

This work was supported by the National Natural Science Foundation of China (grants 41575096 and 41305066), Key Research Program of Frontier Sciences, CA (grants QYZDY-SSW-DQC012) and the National Key Research and Development Program of China (2016YFA0600203). The authors gratefully acknowledge the China Meteorological Administration National Meteorological Information Center for providing the atmospheric forcing data set. We are grateful to the two reviewers for their valuable comments. The daily in situ observation and model outputs are provided as supporting information to this manuscript (Data Sets S1 and S2, respectively).

## References

Baldocchi, D. (1997), Measuring and modelling carbon dioxide and water vapour exchange over a temperate broad-leaved forest during the 1995 summer drought, *Plant Cell Environ.*, *20*(9), 1108–1122, doi:10.1046/j.1365-3040.1997.d01-147.x.

Baldocchi, D. (2008), 'Breathing' of the terrestrial biosphere: Lessons learned from a global network of carbon dioxide flux measurement systems, *Aust. J. Bot.*, *56*(1), 1–26, doi:10.1071/BT07151.

Beer, C., et al. (2009), Temporal and among-site variability of inherent water use efficiency at the ecosystem level, *Global Biogeochem. Cycle*, *23*, 4184–4188, doi:10.1029/2008GB003233.

Beer, C., et al. (2010), Terrestrial gross carbon dioxide uptake: Global distribution and covariation with climate, *Science*, *329*(5993), 834–838, doi:10.1126/science.1184984.

Bonan, G. B. (2008), Forests and climate change: Forcings, feedbacks, and the climate benefits of forests, *Science*, *320*(5882), 1444–1449, doi:10.1126/science.1155121.

Cowan, I. R., and G. D. Farquhar (1977), Stomatal function in relation to leaf metabolism and environment, *Symp. Soc. Exp. Biol.*, *31*, 471–505.

Cox, P. M., D. Pearson, B. B. Booth, P. Friedlingstein, C. Huntingford, C. D. Jones, and C. M. Luke (2013), Sensitivity of tropical carbon to climate change constrained by carbon dioxide variability, *Nature*, *494*(7437), 341–344, doi:10.1038/nature11882.

Dai, A. (2013), Increasing drought under global warming in observations and models, *Nature Clim. Change*, *3*(1), 52–58, doi:10.1038/nclimate1633.

Granier, A., et al. (2007), Evidence for soil water control on carbon and water dynamics in European forests during the extremely dry year: 2003, *Agric. For. Meteorol.*, *143*, 123–145, doi:10.1016/j.agrformet.2006.12.004.

Hudiburg, T. W., S. Luyssaert, P. E. Thornton, and B. E. Law (2013), Interactive effects of environmental change and management strategies on regional forest carbon emissions, *Environ. Sci. Technol.*, *47*(22), 13,132–13,140, doi:10.1021/es402903u.

Hunt, J. E., F. M. Kelliher, T. M. McSeveny, and J. N. Byers (2002), Evaporation and carbon dioxide exchange between the atmosphere and a tussock grassland during a summer drought, *Agric. For. Meteorol.*, *111*(1), 65–82, doi:10.1016/S0168-1923(02)00006-0.

Jia, B., Z. Xie, A. Dai, C. Shi, and F. Chen (2013), Evaluation of satellite and reanalysis products of downward surface solar radiation over East Asia: Spatial and seasonal variations, *J. Geophys. Res. Atmos.*, *118*, 3431–3446, doi:10.1002/jgrd.50353.

Jia, B., Z. Xie, Y. Zeng, L. Wang, Y. Wang, J. Xie, and Z. Xie (2015), Diurnal and seasonal variations of $CO_2$ fluxes and their climate controlling factors for a subtropical forest in Ningxiang, *Adv. Atmos. Sci.*, *32*(4), 553–564, doi:10.1007/s00376-014-4069-4.

Joo, S. J., S. U. Park, M. S. Park, and C. S. Lee (2012), Estimation of soil respiration using automated chamber systems in an oak (*Quercus mongolica*) forest at the Nam-San site in Seoul, Korea, *Sci. Total Environ.*, *416*, 400–409, doi:10.1016/j.scitotenv.2011.11.025.

Keenan, T., R. García, A. D. Friend, S. Zaehle, C. Gracia, and S. Sabate (2009), Improved understanding of drought controls on seasonal variation in Mediterranean forest canopy $CO_2$ and water fluxes through combined in situ measurements and ecosystem modelling, *Biogeosciences*, *6*(8), 1423–1444, doi:10.5194/bg-6-1423-2009.

Keenan, T., S. Sabate, and C. Gracia (2010), Soil water stress and coupled photosynthesis-conductance models: Bridging the gap between conflicting reports on the relative roles of stomatal, mesophyll conductance and biochemical limitations to photosynthesis, *Agric. For. Meteorol.*, *150*, 443–453.

Kotz, S., and S. Nadarajah (2000), *Extreme Value Distributions: Theory and Applications*, Imperial College Press, London.

Krinner, G., N. Viovy, N. de Noblet-Ducoudré, J. Ogée, J. Polcher, P. Friedlingstein, P. Ciais, S. Sitch, and I. C. Prentice (2005), A dynamic global vegetation model for studies of the coupled atmosphere-biosphere system, *Global Biogeochem. Cycle*, *19*, GB1015, doi:10.1029/2003GB002199.

Law, B. E., et al. (2002), Environmental controls over carbon dioxide and water vapor exchange of terrestrial vegetation, *Agric. For. Meteorol.*, *113*(1), 97–120, doi:10.1016/S0168-1923(02)00104-1.

Le Quéré, C., et al. (2013), The global carbon budget 1959–2011, *Earth Syst. Sci. Data*, *5*(1), 165–185, doi:10.5194/essd-5-165-2013.
LeComte, D. (2014), International weather highlights 2013: Super Typhoon Haiyan, super heat in Australia and China, a long winter in Europe, *Weatherwise*, *67*(3), 20–27, doi:10.1080/00431672.2014.899800.
Liu, J., Z. Xie, B. Jia, X. Tian, P. Qin, J. Zou, Y. Yu, Q. Sun, Y. Wang, and J. Xie (2013), The long-term field experiment observatory and preliminary analysis of land-atmosphere interaction over hilly zone in the subtropical monsoon region of southern China, *Atmos. Oceanic. Sci. Lett.*, *6*, 203–209, doi:10.3878/j.issn.1674-2834.13.0112.
Liu, Y., G. Yu, X. Wen, Y. Wang, X. Song, J. Li, X. Sun, F. Yang, Y. Chen, and Q. Liu (2006), Seasonal dynamics of $CO_2$ fluxes from subtropical plantation coniferous ecosystem, *Sci. China Earth Sci.*, *49*(2), 99–109, doi:10.1007/s11430-006-8099-3.
Lloyd, J., and J. A. Taylor (1994), On the Temperature Dependence of Soil Respiration, *Funct. Ecol.*, *8*(3), 315–323.
Loreto, F., and M. Centritto (2008), Leaf carbon assimilation in a water-limited world, *Plant Biosyst.*, *142*(1), 154–161, doi:10.1080/11263500701872937.
Oleson, K. W., et al. (2013), Technical description of version 4.5 of the Community Land Model (CLM), *Rep. NCAR/TN-503 + STR*, 420.
Pan, Y., et al. (2011), A large and persistent carbon sink in the world's forests, *Science*, *333*, 988–993, doi:10.1126/science.1201609.
Reichstein, M., et al. (2005), On the separation of net ecosystem exchange into assimilation and ecosystem respiration: Review and improved algorithm, *Global Change Biol.*, *11*(9), 1424–1439, doi:10.1111/j.1365-2486.2005.001002.x.
Reichstein, M., et al. (2007), Reduction of ecosystem productivity and respiration during the European summer 2003 climate anomaly: A joint flux tower, remote sensing and modelling analysis, *Global Change Biol.*, *13*(3), 634–651, doi:10.1111/j.1365-2486.2006.01224.x.
Reichstein, M., et al. (2013), Climate extremes and the carbon cycle, *Nature*, *500*(7462), 287–295, doi:10.1038/nature12350.
Sakaguchi, K., X. Zeng, B. J. Christoffersen, N. Restrepo-Coupe, S. R. Saleska, and P. M. Brando (2011), Natural and drought scenarios in an east central Amazon forest: Fidelity of the Community Land Model 3.5 with three biogeochemical models, *J. Geophys. Res.*, *116*, G01029, doi:10.1029/2010JG001477.
Saleska, S. R., et al. (2003), Carbon in Amazon forests: Unexpected seasonal fluxes and disturbance-induced losses, *Science*, *302*(5650), 1554–1557, doi:10.1126/science.1091165.
Schlesinger, W. H., and S. Jasechko (2014), Transpiration in the global water cycle, *Agric. For. Meteorol.*, *189*, 115–117, doi:10.1016/j.agrformet.2014.01.011.
Shi, C., Z. Xie, H. Qian, M. Liang, and X. Yang (2011), China land soil moisture EnKF data assimilation based on satellite remote sensing data, *Sci. China Earth Sci.*, *54*, 1430–1440, doi:10.1007/s11430-010-4160-3.
Sun, X., X. Wen, G. Yu, Y. Liu, and Q. Liu (2006), Seasonal drought effects on carbon sequestration of a mid-subtropical planted forest of southeastern china, *Sci. China Earth Sci.*, *49*(S2), 110–118.
Thornton, P. E., and N. A. Rosenbloom (2005), Ecosystem model spin-up: Estimating steady state conditions in a coupled terrestrial carbon and nitrogen cycle model, *Ecol. Model.*, *189*, 25–48, doi:10.1016/j.ecolmodel.2005.04.008.
Van der Molen, M. K., et al. (2011), Drought and ecosystem carbon cycling, *Agric. For. Meteorol.*, *151*(7), 765–773, doi:10.1016/j.agrformet.2011.01.018.
Wang, L., W. Chen, and W. Zhou (2014), Assessment of future drought in Southwest China based on CMIP5 multimodel projections, *Adv. Atmos. Sci.*, *31*(5), 1035–1050, doi:10.1007/s00376-014-3223-3.
Webb, E. K., G. I. Pearman, and R. Leuning (1980), Correction of flux measurements for density effects due to heat and water vapour transfer, *Q. J. R. Meteor. Soc.*, *106*(447), 85–100, doi:10.1002/qj.49710644707.
Wen, X., H. Wang, G. Yu, and X. Sun (2010), Ecosystem carbon exchange of a subtropical evergreen coniferous plantation subjected to seasonal drought, 2003–2007, *Biogeosciences*, *7*(1), 357–369, doi:10.5194/bg-7-357-2010.
Wilczak, J., S. P. Oncley, and S. A. Stage (2001), Sonic anemometer tilt correction algorithms, *Bound-lay. Meteorol.*, *99*(1), 127–150, doi:10.1023/A:1018966204465.
Yu, G., X. Song, Q. Wang, Y. Liu, D. Guan, J. Yan, X. Sun, L. Zhang, and X. Wen (2008), Water-use efficiency of forest ecosystems in eastern China and its relations to climatic variables, *New Phytol.*, *177*(4), 927–937, doi:10.1111/j.1469-8137.2007.02316.x.
Yuan, X., Z. Ma, M. Pan, and C. Shi (2015), Microwave remote sensing of short-term droughts during crop growing seasons, *Geophys. Res. Lett.*, *42*, 4394–4401, doi:10.1002/2015GL064125.
Zeng, N., H. Qian, C. Roedenbeck, and M. Heimann (2005), Impact of 1998–2002 midlatitude drought and warming on terrestrial ecosystem and the global carbon cycle, *Geophys. Res. Lett.*, *32*, L22709, doi:10.1029/2005GL024607.
Zhou, S., B. Yu, Y. Huang, and G. Wang (2015), Daily underlying water use efficiency for AmeriFlux sites, *J. Geophys. Res. Biogeosci.*, *120*, 887–902, doi:10.1002/2015JG002947.
Zhu, Z., X. Sun, X. Wen, Y. Zhou, J. Tian, and G. Yuan (2006), Study on the processing method of nighttime $CO_2$ eddy covariance flux data in ChinaFLUX, *Sci. China Earth Sci.*, *49*(2), 36–46, doi:10.1007/s11430-006-8036-5.